



Deposited via The University of Sheffield.

White Rose Research Online URL for this paper:

<https://eprints.whiterose.ac.uk/id/eprint/232500/>

Version: Accepted Version

Article:

Qiu, L., Daniell, T.J., Nafees, M. et al. (2025) Biochar-induced strong microbial carbon limitation prompts organic carbon sequestration and plant growth in antibiotic-contaminated soil. *Plant and Soil*, 516 (2). pp. 2293-2309. ISSN: 0032-079X

<https://doi.org/10.1007/s11104-025-07861-1>

© 2025 The Authors. Except as otherwise noted, this author-accepted version of a journal article published in *Plant and Soil* is made available via the University of Sheffield Research Publications and Copyright Policy under the terms of the Creative Commons Attribution 4.0 International License (CC-BY 4.0), which permits unrestricted use, distribution and reproduction in any medium, provided the original work is properly cited. To view a copy of this licence, visit <http://creativecommons.org/licenses/by/4.0/>

Reuse

This article is distributed under the terms of the Creative Commons Attribution (CC BY) licence. This licence allows you to distribute, remix, tweak, and build upon the work, even commercially, as long as you credit the authors for the original work. More information and the full terms of the licence here: <https://creativecommons.org/licenses/>

Takedown

If you consider content in White Rose Research Online to be in breach of UK law, please notify us by emailing eprints@whiterose.ac.uk including the URL of the record and the reason for the withdrawal request.

1 **Biochar-induced strong microbial carbon limitation prompts**
2 **organic carbon sequestration and plant growth in antibiotic-**
3 **contaminated soil**

4

5 *Linlin Qiu^a, Tim J. Daniell^b, Muhammad Nafees^c, Yihao Chen^d, Shuyu Zhou^e, Weihong*

6 *Wu^a, Jia Du^a, Qingwei Zhou^a, Meiqing Jin^a, Weiyang Ji^f, Jiaying Ge^f, Hongyan Guo^{c,g*}*

7

8 ^a College of Materials and Environmental Engineering, Hangzhou Dianzi University,
9 Hangzhou, Zhejiang, 310012, China.

10 ^b School of Biosciences, University of Sheffield, Sheffield S10 2TN, UK

11 ^c State Key Laboratory of Pollution Control and Resource Reuse, School of the
12 Environment, Nanjing University, Nanjing, Jiangsu, 210023, China.

13 ^d College of Chemical Engineering, Beijing University of Chemical Technology,
14 Beijing, 100029, China.

15 ^e Shangyu Branch of Shaoxing Ecological Environment Bureau, Shaoxing, Zhejiang,
16 312300, China.

17 ^f Zhejiang Provincial Cultivated Land Quality and Fertilizer Administration Station,
18 Hangzhou, Zhejiang, 310020, China.

19 ^g Quanzhou Institute of Environmental Protection Industry, Nanjing University,
20 Quanzhou, Fujian, 362000, China.

21 * Corresponding author. Tel.: +86-25-89680263; Fax: +86-25-89680263.

22 E-mail address: hyguo@nju.edu.cn (H. Guo).

23 **Abstract**

24 *Background and aims* Organic fertilization introduces considerable antibiotics into
25 agricultural soil. Biochar has been widely proposed as a win-win strategy for enhancing
26 soil health, achieving carbon neutrality and improving plant growth. However, the
27 mechanisms of how biochar enhances carbon sequestration and stimulates plant
28 development have not been fully characterized, especially in soil containing antibiotics.

29 *Methods* As such, a greenhouse experiment was conducted to investigate the microbial-
30 driven pathways by which biochar enhances soil carbon stabilization and
31 synergistically improves plant productivity. Amplicon sequencing was adopted to
32 analyze soil microbial community composition and untargeted metabolomics was used
33 to understand the molecular composition of soil microbial metabolites.

34 *Results* High-temperature woody biochar increased soil organic carbon content by
35 almost 50%, while the dissolved organic carbon was reduced by half. This induced
36 substantial microbial carbon limitation, decreasing microbial biomass carbon content
37 and reducing microbial carbon metabolism capability. Sulfadiazine presence could
38 enhance biochar-induced microbial carbon limitation and has more serious impacts on
39 soil microbial community. 107 soil metabolites changed significantly after biochar
40 application. Enrichment analysis indicated that biochar application potentially
41 disturbed ABC transporters and amino acid metabolism. The increased content of
42 compounds associated with mineral and organic ion transports might promote nutrient
43 retention in soil, leading to greater accumulation of photosynthetic pigments and
44 increased ryegrass growth.

45 *Conclusions* We found that biochar-induced strong microbial carbon limitation prompts
46 organic carbon sequestration and plant growth in antibiotic-contaminated soil.
47 Understanding the intrinsic relationship between biochar-mediated soil microbial
48 metabolism and plant growth will facilitate the advancement of low-input, high-
49 resilience sustainable agriculture.

50 **Keywords:** biochar, antibiotic, soil organic matter, soil microbial community, carbon
51 sequestration

52 **1. Introduction**

53 Soil constitutes the most significant terrestrial organic carbon sink, containing more
54 organic carbon than global vegetation and the atmosphere combined (Paustian et al.
55 2016). Thus, even a tiny loss of soil organic carbon (SOC) stocks could substantially
56 influence atmospheric CO₂ levels, leading to further global climate warming (Paustian
57 et al. 2016; Moinet et al. 2023). Agricultural soil generally has higher percent SOC
58 losses and is a key SOC pool that can be influenced through wise soil management to
59 increase carbon sequestration, and remit emissions of greenhouse gas (Sanderman et al.
60 2017; Guenet et al. 2021). As intensive farming and sustainable agriculture advance,
61 however, many antibiotics are introduced into agricultural soils through organic
62 fertilizer application (Liu et al. 2024). The continuous accumulation of antibiotics held
63 the potential to interfere SOC stock through influencing soil microbial community and
64 metabolism process (Qiu et al. 2021). Given agriculture's vital role in climate mitigation,
65 prioritizing efficient soil carbon sequestration strategies that account for antibiotic
66 impacts is essential for achieving carbon neutrality.

67 Biochar has been extensively advocated as a win-win strategy to achieve carbon
68 sequestration and immobilize contaminants (Luo et al. 2023). Biochar can potentially
69 moderate native SOC decomposition through positive, neutral, or adverse priming
70 effects to influence carbon sequestration (Maestrini et al. 2014). The composition of
71 biochar and SOC, nutrient availability, and microorganisms are the main drivers of
72 controlling the direction of priming effects (Luo et al. 2023). For example, low-
73 temperature biochar is abundant in labile organic carbon, which can stimulate soil

74 microorganisms growth and expedite the decomposition of SOC with positive priming
75 effects in the short term (Kuzyakov 2010; Ren et al. 2022). However, adverse priming
76 effects frequently arise from the suppression of soil microorganisms, whether due to
77 microbial C limitation induced by sorption-reduced labile C availability or due to direct
78 toxicity from noxious biochar substances. Significantly, biochar-induced increased
79 competition between keystone taxa can also lead to adverse priming effects enabling
80 SOC sequestration, even though biochar application typically stimulates the soil
81 microorganism biomass and diversity (Chen et al. 2019). Current studies fail to
82 reconcile these contradictory mechanisms and establish consistent conclusions
83 regarding the long-term implications of biochar application for native SOC persistence.
84 Porous structure and large specific surface area endow biochar with a substantial
85 adsorption property, effectively immobilizing antibiotics. Han et al. (2024) found that
86 biochar significantly reduced antibiotic availability in soil, concurrently reshaping soil
87 microbial community composition. In contrast, there is also some evidence that shows
88 biochar-sorbed antibiotics retain bioavailability for soil microbes (Wang et al., 2020).
89 Moreover, Qiu et al. (2025) indicated that antibiotic-induced disturbances to soil
90 microbial structure and function still exist after biochar application. Consequently,
91 reconciling biochar's dual effects on antibiotic bioavailability and microbial resilience
92 remains critical for deploying it as a reliable carbon sequestration enhancer in
93 antibiotic-polluted soils.

94 Although biochar has been demonstrated to be a strong candidate to aid an increase in
95 carbon sequestration and pollution immobilization, deep insight into the mechanisms

96 underlying C cycling and sequestration remains largely unexplored, especially in
97 antibiotic-contaminated soils. In general, the core issue required to allow a
98 comprehensive evaluation of biochar's potential and feasibility as a carbon
99 sequestration strategy hinges on its impact on the molecular composition and speciation
100 of indigenous organic carbon. However, soil organic carbon turnover exploration has
101 been restricted by SOC chemical complexity and spatial heterogeneity. As a nascent
102 technology, soil metabolomics shows potential to provide a greater understanding of
103 carbon cycling. Untargeted soil metabolomics offers a global analysis of specific
104 metabolites of low molecular weight (<1000 Da), allowing the identification of
105 molecular networks and cellular pathways. Studies have confirmed that this approach
106 elucidates key biological mechanisms in terrestrial carbon cycling (Swenson et al. 2015;
107 Withers et al. 2020).

108 To sum up, biochar demonstrates promise for regulating soil carbon cycling and
109 facilitating pollution remediation. However, existing research predominantly focuses
110 on uncontaminated soil. A critical gap remains regarding how biochar, specifically
111 within the stressful context of antibiotic-contaminated soil, influences core ecological
112 processes of SOM turnover. Based on our current understanding, we hypothesize that
113 antibiotic would influence SOM composition through affecting soil microbial
114 community composition and function. Biochar application would induce distinct shifts
115 in SOM composition in antibiotic-contaminated soil compared to uncontaminated
116 controls, mediated through microbial community restructuring and functional
117 adaptation. To test these hypotheses and address this gap, a pot experiment was

118 designed to: (i) investigate the mechanisms by which biochar addition alters the content
119 and chemical composition of SOM in antibiotic-contaminated versus uncontaminated
120 soil; (ii) elucidate biochar-driven shifts in soil bacterial community structure, diversity,
121 and carbon-cycling functional traits under antibiotic stress; (iii) decipher the interactive
122 mechanisms through which biochar enhances carbon sequestration efficiency and
123 stimulates plant development in antibiotic-impacted soil systems.

124 **2. Material and methods**

125 **2.1 Experiment design**

126 Topsoil classified as Anthrosol was collected from a farmland in Zhejiang province,
127 China (29°47' N, 121°21' E). Detailed information about the soil is shown in Table S1.
128 A given mass of sulfadiazine (SDZ) was added to the air-dried soil to attain a final
129 concentration of 5 mg kg⁻¹. This set concentration is comparable to the concentrations
130 found in agricultural soil near feedlots (Ji et al., 2012), representing a relatively high
131 field condition. The biochar employed in this investigation was synthesized through a
132 standardized pyrolysis protocol. Air-dried sawdust underwent a slow pyrolysis process
133 with a heating rate of 15 °C min⁻¹ to a terminal temperature of 500°C, maintained for
134 2 hours in a muffle furnace under oxygen-limited conditions using continuous flowing
135 N₂ as the medium gas. The biochar was mechanically ground and passed through a 2-
136 mm mesh sieve before use. The basic physicochemical properties were displayed in
137 Table S2 and Fig. S1 in the supplementary material. Biochar was mixed with the above
138 two soils in a proportion of 3:100 (mass ratio). Then, 100 g soil or the mixture of soil
139 and biochar was packed into plastic containers to yield control (CK: 0 mg kg⁻¹ of SDZ),

140 SDZ addition (SDZ: 5 mg kg⁻¹ of SDZ), biochar addition (B: control soil + 3% biochar),
141 SDZ and biochar addition (SDZB: 5 mg kg⁻¹ of SDZ + 3% biochar) treatment. The
142 experimental design incorporated four biological replicates for each treatment.
143 Ryegrass seeds were disinfected using 10% H₂O₂ solution, washed three times with
144 ddH₂O, and sprouted on autoclaved paper towels for a week. Twenty treated ryegrass
145 seeds with similar growth were transplanted into each pot, and water was added to
146 achieve 60% field capacity. After a 40-day incubation, ryegrass was separated from the
147 soil, and total fresh biomass was determined. Soil samples were collected and
148 subdivided into three discrete aliquots. One was air-dried for basic physicochemical
149 index determination and dissolved organic matter extraction. One was collected and
150 stored at 4 °C for microbial carbon metabolic activity evaluation. The remainder was
151 stored at – 80 °C for soil microbial community and metabolomics analysis.

152 **2.2 Photosynthetic pigments determination**

153 The content of photosynthetic pigments was determined following the protocol of
154 Lichtenthaler (1987). In brief, 0.25 g ryegrass leaf samples were weighted and mixed
155 with 5 mL 80% acetone solution for 12 h in the dark. After centrifugation, the
156 supernatant detects absorbance at 663 nm, 645 nm, and 470 nm using a microplate
157 reader (Varioskan LUX, Thermo Fisher Scientific, Vantaa, Finland).

158 **2.3 Soil organic carbon composition characterization**

159 The Walkley–Black dichromate oxidation technique was employed to quantify the soil
160 organic carbon (SOC) content (Nelson and Sommers 1982). Dissolved organic matter
161 (DOM) was extracted following the protocol described by Oren and Chefetz (2012).

162 DOM quantity was assessed with a TOC analyzer (vario TOC, Elementar, Germany).
163 Fluorescence excitation-emission matrix (EEM) spectroscopy was recorded to assess
164 the composition of soil DOM using a F-7000 fluorescence spectrometer (Hitachi High
165 Technologies, Japan). The fluorescence regional integration technique was employed
166 to evaluate DOM composition (Chen et al. 2003).

167 **2.4 Microbial biomass measurement, sequencing, and bioinformatics examination**

168 The microbial biomass carbon (MBC) content was evaluated by determining the
169 difference in dissolved organic carbon (DOC) between fumigated and unfumigated
170 samples, as measured by a TOC/TN analyzer, with an applied efficiency factor of 0.45
171 (Wu et al. 1990).

172 Mobio DNeasy Powersoil kit (MoBio, Carlsbad, CA, USA) was used to extract
173 microbial DNA from lyophilized soil. After quality and quantity checks, the V3 region
174 of 16S rRNA gene was amplified using a universal primer pair of 341F/518R
175 (Klindworth et al. 2012). The composition and procedure for the amplification mixture
176 were delineated in a prior investigation (Li et al., 2018). After visualization and check,
177 the PCR products were purified, quantified, and pooled for analysis. All amplicons were
178 sequenced by an Ion-Torrent sequencing platform (Life Technologies, USA). After
179 removing low-quality reads, the clean reads were de-noised using the DADA2 method
180 and taxon classification in QIIME2 (v.2019.7) based on the Silva database (Hall and
181 Beiko, 2018; Callahan et al., 2016; Quast et al. 2012).

182 **2.5 Microbial carbon metabolic profiles**

183 The metabolic capability of the soil microbial community was assessed using Biolog

184 EcoPlates (Biolog Inc., Hayward, CA, USA). Soil microbes were extracted according
185 to the procedure provided by Chen et al. (2019). In brief, the mixture comprising fresh
186 soil and sterile saline solution was shaken at 90 rpm for 30 min, followed by a 30-min
187 static period. Subsequently, the diluted supernatant was incubated in Biolog EcoPlates
188 at a temperature of 25°C in darkness for a duration of seven days. Color development
189 reflects carbon utilization monitored by a microplate spectrophotometer (Thermo
190 Scientific, USA) at 590 nm every 24 h.

191 **2.6 Untargeted metabolomics measurement of soil metabolite**

192 Metabolite extraction followed the protocol reported by the previous study (Qiu et al.
193 2021) and described in supplementary data S1. A non-targeted metabolomics
194 investigation was conducted with a gas chromatograph (Agilent 7890B) coupled with
195 a mass selective detector (Agilent 5977A) (Agilent Technologies Inc., CA, USA).
196 Using highly pure helium gas as a carrier, the GC thermal program was 60 °C for 1 min,
197 ramped to 125 °C at a rate of 8 °C min⁻¹, increased to 270 °C at a rate of 5 °C min⁻¹,
198 305 °C at 10 °C min⁻¹ and finally held at 305 °C for 3 min. Mass data was obtained
199 through a full scan from 50 to 500 m/z with 70 eV ionization energy.

200 **2.7 Data and statistical analysis**

201 Statistical comparisons were conducted using one-way analysis of variance (ANOVA)
202 in SPSS 6.0 software (SPSS, Chicago, IL, USA) with Fisher's least significant
203 difference tests. Changes in soil microbial community were assessed by principal
204 coordinate analysis (PCoA, Anderson and Willis 2003), and the statistical significance
205 was assessed by a permutational multivariate analysis of variance (PERMANOVA,

206 Anderson 2001). STAMP software was employed to investigate the dissimilarity in the
207 microbial community because of biochar addition using Welch's t-test between two
208 groups with Benjamini-Hochberg FDR correction (Parks et al. 2014). Statistical
209 analyses of the untargeted metabolomic analyses were processed using MetaboAnalyst
210 4.0 (Chong et al. 2019). Sparse Partial Least Squares Discriminant Analysis (sPLS-DA)
211 was performed in R (v.4.2.2) using the function "splsga" from the mixOmics package
212 (v.6.22.0). The model was configured with the number of components (*ncomp*) set to 2
213 and the number of variables retained per component (*keepX*) fixed at 10, with repeated
214 random resampling. Enrichment analysis was carried out based on differential
215 metabolites caused by biochar addition were analyzed with the help of MB role 2.0
216 (López-Ibáñez et al. 2016).

217 **3. Results**

218 **3.1 Impact of biochar application and SDZ presence on ryegrass growth**

219 After 40 days of incorporation, both biochar application and SDZ presence improved
220 the growth and development of ryegrass. The fresh biomass of ryegrass increased
221 significantly from 3.66 (\pm 0.3) g in control to 5.46 (\pm 0.2) g in SDZ treatment, 7.68 (\pm
222 0.7) g in sole biochar treatment, and 6.62 (\pm 0.6) g in SDZB treatment ($P < 0.05$, Fig.
223 1a). In comparison to the control group, the application of biochar resulted in a
224 significant increase ($P < 0.05$) in the root length of ryegrass, irrespective of whether the
225 soil contained SDZ or not (Fig. 1b). Moreover, the photosynthetic pigments were
226 significantly higher in the sole biochar treatment ($P < 0.05$, Fig. 1c). Specifically, the
227 biochar-induced increase in chlorophyll a, chlorophyll b and carotenoids was 18.1%,

228 33.3% and 36.7% respectively. Single SDZ presence significantly increased the content
229 of chlorophyll b and carotenoids, while this trend disappeared after biochar application.

230 **3.2 Shift in soil organic carbon due to biochar application and SDZ presence**

231 Our results demonstrated that biochar application raised SOC levels, both in the
232 presence and absence of SDZ in the soil (Fig. 2a). The control contained 20.97 (\pm 1.31)
233 g C kg⁻¹ soil, the sole biochar treatment stored 37.93 (\pm 1.26) g C kg⁻¹ soil and the
234 SDZB treatment contained 41.07 (\pm 1.34) g C kg⁻¹ soil, almost double that of the control.
235 Whereas the DOM content was significantly reduced from 99.43 (\pm 5.56) to 55.55 (\pm
236 2.91) mg kg⁻¹ by half due to sole biochar application (Fig. 2b). To extend understanding
237 of DOM variation, we assessed differences in composition. As shown in Fig S2, visible
238 changes occurred in DOM composition after biochar addition. Fluorescent region
239 integral analysis demonstrated that humic acid-like substances were the predominant
240 component of DOM in both the control (58.00%-65.92%) and SDZ treatment (47.43%-
241 54.61%), whilst the distribution was more balanced after biochar application (Fig. 2c).
242 Compared to the control, protein-like substance content exhibited a 1.32-fold elevation
243 under biochar treatment. When antibiotics were introduced to the soil, the enhancement
244 effect of biochar was further intensified, achieving a 2.5-fold increase in protein-like
245 substance levels. Meantime, biochar caused an increase of approximately 50% in the
246 proportion of both fulvic acid-like substances and soluble microbial byproduct-like
247 substances. In contrast, a decline of 57.33% and 44.05% in humic-like substances was
248 observed in biochar-treated control soil and SDZ-contaminated soil, respectively. To
249 sum up, high-temperature woody biochar application lifted the SOC ceiling, reduced

250 the DOC content and promoted humic-like substance sequestration.

251 **3.3 Biochar modifies soil bacterial composition and carbon metabolic ability in** 252 **SDZ-amended and non-amended soils**

253 Microbial biomass carbon (MBC) was significantly reduced ($P < 0.05$) after biochar
254 application, especially for soil with the presence of SDZ (Fig. 3a). No significant
255 change was found in the microbial Shannon diversity index in sole biochar treatment,
256 while it decreased significantly in SDZB treatment (Fig. 3b). A PCoA analysis showed
257 a clear separation in the first dimension between the four treatments (Fig. 3c), and
258 PERMANOVA confirmed a significant change in the microbial community because of
259 biochar application ($P < 0.05$).

260 To get an insight into microbial community alternation, variations in microbial
261 community composition at the taxonomic level were considered (Fig. 3d). The majority
262 of bacterial ASVs were assigned to *Proteobacteria* (relative abundance ~ 34.4-22.8%)
263 and *Actinobacteria* (relative abundance ~ 45.7.0-31.1%). Compared to control,
264 *Proteobacteria* and *Patescibacteria* were enriched after biochar application ($P < 0.05$).
265 Conversely, a pronounced decrease was detected in the relative abundance of
266 *Actinobacteria* and *Gemmatimonadetes* ($P < 0.05$) in sole biochar application treatment.
267 Moreover, there was a significant decrease in the relative abundance of *Chloroflexi* in
268 SDZB treatment ($P < 0.05$). When assessing on an individual ASV basis 12 ASVs show
269 significant differences between control and B treatment (Fig. 3e). ASVs assigned to
270 *Bdellovibrio* (genus level, $P < 0.05$), *Fibrobacteraceae*, *Sphingomonadaceae* and
271 *Rhodobacteraceae* (family level, all $P < 0.01$), OPB56 (order level, $P < 0.01$) and

272 *Gammaproteobacteria* (class level, $P < 0.01$) increased in relative abundance with
273 biochar addition. In contrast, ASVs assigned to *Acidobacteria* (phylum level, $P < 0.01$),
274 *Burkholderiaceae*, *Thermoanaerobaculaceae* and *Caulobacteraceae* (family level, all
275 $P < 0.05$) as well as *Solirubrobacterales* (order level, $P < 0.01$) significantly decreased
276 in relative abundance. In addition, SDZB treatment resulted in a statistically significant
277 alteration in the relative abundance of 7 ASVs compared to the control (Fig. 3f).
278 Specifically, ASVs assigned to *Solirubrobacterales* (order level, $P < 0.01$), *Opitutaceae*,
279 *Pedosphaeraceae*, and *Caulobacteraceae* (family level, all $P < 0.05$) decreased in
280 abundance under SDZB treatment. In contrast, ASVs assigned to *Saccharimonadales*
281 (order level, $P < 0.01$) and *Anaeromyxobacter* (genus level, $P < 0.01$) increased in
282 relative abundance under SDZB treatment.

283 The total microbial carbon metabolism capability was significantly decreased in B,
284 SDZ, and SDZB treatments (Fig. 4a, $P < 0.05$) with significant shifts in the respiration
285 of specific carbon compound classes. Carboxylic acids, amino acids, amines, and
286 polymers showed significantly reduced activity in B, SDZ, and SDZB treatments (Fig.
287 4a, $P < 0.05$). The metabolic activity of utilizing phenolic acids increased considerably
288 in B treatment, however, it decreased under SDZ and SDZB treatments (Fig. 4a, $P <$
289 0.05). In addition, sole biochar application did not induce changes in the utilization of
290 carbohydrates, while a significant decrease was found in SDZB treatment. Additionally,
291 SDZ induced a significant decline in normalized total microbial carbon metabolic
292 ability, while there was no significant change in B and SDZB treatment (Fig. 4b). The
293 normalized metabolic activity of utilizing carbohydrates increased significantly in B

294 and SDZB treatment. In contrast, both SDZ addition and biochar application could
295 induced a noticeable decrease in the normalized metabolic activity of utilizing amino
296 acids and amines (Fig. 4b, $P < 0.05$).

297 **3.4 Variation in soil metabolites owing to biochar application and SDZ presence**

298 A total of 262 soil metabolites were recognized through GC-QTOF-MS analysis. These
299 soil metabolites primarily related to amines, amino acids, carbohydrates, fatty acids,
300 and organic acids (Fig. 5). Results showed that carbohydrates were dominant,
301 accounting for 35.5% - 53.6% in all four treatments (Fig. 5a). Moreover, an apparent
302 decrease in the relative contribution of carbohydrates were detected after biochar
303 application. In contrast, the rising relative content of amino acids and amines after
304 biochar application was related to the suggested decreased microbial capability to
305 utilize these two classes demonstrated by the Biolog EcoPlates (Fig. 4). A sparse partial
306 least-squares discriminant analysis (sPLS-DA) indicated metabolites from a single SDZ
307 presence treatment grouped with those from the control soil. At the same time, there
308 was an apparent separation in metabolites from B and SDZB treatment in the first
309 component, explaining 25.4% of the variance (Fig. 5f). Analysis of the loadings of PLS-
310 DA suggested that adenosine (nucleosides), gondoic acid (fatty acids), glycerol
311 (carbohydrates) and salicylaldehyde (amino acids) was the dominant compounds
312 driving the separation.

313 More specifically, SDZ presence and biochar addition induced significant alternations
314 in the content of 107 soil metabolites (Table S3, $P < 0.05$). Hierarchical cluster analysis
315 further investigated the variation in soil metabolites. The heatmap covered the top 50

316 list of differential metabolites, shown in three clear clusters (Fig. 6). Cluster 1 mainly
317 contained amino acids, carbohydrates, and amines, which had an increased relative
318 content after biochar application. Specifically, biochar application increased the relative
319 content of L-glutamic acid (map00480, map00970, and map00910), 5,6-dihydrouracil
320 (map00410), and putrescine (map02010, map00480, and map00330). Within the largest
321 cluster (cluster 2), 20 compounds were under-represented after biochar application. It
322 mainly consisted of fatty acids, organic acids, and carbohydrates, with few amino acids.
323 The relative content of palmitic acid, palmitoleic acid, and myristic acid was
324 significantly decreased after biochar application, and these metabolites play an essential
325 role in fatty acid biosynthesis (map00061). Compounds in cluster 3 were the key factors
326 driving the differences between B and SDZB treatment, and organic acids were the
327 main constituents. Compared to a single biochar application, SDZ presence produced a
328 noteworthy reduction in the relative contents of glycolic acid (map00361), oxalic acid
329 (map00230), and 2-ketobutyric acid (map00290). Through enrichment analysis, we
330 found that these distinct compounds on the KEGG map were significantly involved in
331 ABC transporters (map02010), glutathione metabolism (map00480), and amino acids
332 metabolisms (map00410, map00330, map00250, map00290 and map00270) (Table S4,
333 Fig.7). Moreover, most of the metabolites related to mineral and organic ion transports
334 were up-regulated. In contrast, compounds involved in phosphate and amino acid
335 transporters were down-regulated in sole biochar application. Taken together, biochar
336 application potentially disturbed the transport and metabolism of amino acids, resulting
337 in a significantly elevated content in the soil.

338 **4. Discussion**

339 **4.1 SDZ presence enhanced biochar-driven microbial carbon limitation**

340 As the most biologically accessible component of SOC, soil DOC exhibits a rapid
341 turnover rate and plays a crucial role in regulating soil CO₂ emissions (Chen et al.,
342 2023). As an exogenous organic carbon source, biochar can regulate soil DOC turnover
343 by applying additional DOC or adsorption of existing easily respirable DOC,
344 influencing soil microbial processing through limitation. Biochar amendments are
345 expected to increase soil DOC content because biochar usually contains a significant
346 level of DOC, especially when produced at lower temperature (Liu et al. 2022a).
347 Unsurprisingly it has been previously confirmed that soil DOC content significantly
348 increased after addition of low-temperature biochar boosting soil microbial growth with
349 associated and triggering of short-term positive priming effects (Ren et al., 2022; Chen
350 et al., 2023).

351 In contrast, in this study using high temperature biochar soil DOC content was reduced
352 approximately two-fold by addition (Fig. 2b), in line with with other studies that also
353 found a decrease in DOC content when adding high-temperature produced biochar
354 (Yang et al. 2022a, b). The decrease may associate with the porous structure of biochar,
355 which may provide effective adsorption sites for soil DOC (Feng et al. 2021). High-
356 temperature biochar usually exhibits a relatively high adsorption potential toward
357 organic matter (Kasozi et al. 2010). Similarly, Guo et al. (2020) also indicated that high-
358 temperature biochar caused a lowered soil DOC due to stronger carbon limitation.
359 Moreover, Chen et al. (2022) suggested that woody biochar can cause stronger

360 microbial carbon limitation than crop residue biochar. The woody biochar produced at
361 500 °C used in our study possesses large surface areas (S_{BET} : $525.28 \pm 18.20 \text{ m}^2/\text{g}$, Table
362 S2), porous structure, and various functional groups (Fig. S1), expected to have strong
363 adsorption of organic matter.

364 More importantly, DOC content significantly decreased in SDZB treatment compared
365 to the B treatment. The behind reason might be that antibiotic inhibited microbial
366 activity and weaken DOC decomposition, leading to temporary accumulation of DOC.

367 This excess DOC can be adsorbed by biochar and immobilized as non-extractable forms,
368 thereby decreasing measurable DOC concentrations. Additionally, antibiotic stress
369 forces soil microbes into a "maintenance metabolism" state, diverting energy to
370 resistance mechanisms instead of growth. Consequently, less DOC is converted into
371 microbial biomass, increasing the pool of DOC immobilized through biochar
372 adsorption. Our results suggested that SDZ presence can enhance biochar-induced
373 microbial carbon limitation.

374 **4.2 Strong microbial carbon limitation caused significant alternations in soil** 375 **bacterial community composition and fuction**

376 Although high-temperature biochar, such as that used in this study, offers more
377 habitable space for many soil microbes, its limited available labile carbon substrates
378 resulted in a reduced overall population size (Fig. 3a). Single biochar application
379 induced the shift in the soil microbial community composition by stimulating the
380 relative abundance of *Proteobacteria* and *Patescibacteria*, in agreement with the
381 findings reported in previous studies (Liu et al. 2022b; Lu et al. 2020; Gao et al. 2017).

382 Through further analysis, we found that *Gammaproteobacteria* (class level),
383 *Sphingomonadaceae* and *Rhodobacteraceae* (family level), and *Bdellovibrio* (genus
384 level) were the main contributors to the increased relative abundance of *Proteobacteria*
385 (Fig. 3c). Biochar can provide shelter to *Proteobacteria* for its colonization, growth,
386 and multiplication (Tan et al. 2022). *Rhodobacteraceae* involved in soil carbon and
387 nitrogen cycle (Fortuna et al. 2011), and its increased relative abundance indicated a
388 direct impact of biochar application on SOM turnover. *Burkholderiaceae* (order
389 *Burkholderiales*) includes opportunistic pathogens and can cause severe disease
390 (Rhodes and Schweizer 2016), and *Bdellovibrio* are versatile predatory bacteria with
391 great potential as antimicrobial agents (Oyedara et al. 2018). The increased relative
392 abundance of the genus *Bdellovibrio* and decreased relative abundance of the order
393 *Burkholderiaceae* provided support for the potential capability of biochar in mitigating
394 soil-borne pathogens. Moreover, our results displayed a significant decrease in the
395 relative abundance of *Actinobacteria* and *Gemmatimonadetes*, as reported by previous
396 studies (Gao et al. 2017; Li et al. 2022). *Actinobacteria* serves as a consumer of carbon-
397 rich and recalcitrant substances, while *Gemmatimonadetes* exhibit potential as
398 degraders of recalcitrant carbon compounds (Lehmann et al. 2011). The significant
399 decrease in the relative abundance of these soil recalcitrant carbon-degrading microbes
400 hold the potential to promote SOC stabilization. In addition, biochar-mediated
401 alterations to soil properties (e.g., porosity, pH, cation exchange capacity) can also drive
402 shifts in microbial community composition. There was a significant decrease in the
403 relative abundance of the phylum *Acidobacteria*. It might relate to the higher pH in

404 biochar treatment, which is unfavorable for its growth (Table S5).

405 Compared to sole biochar application, MBC significantly decreased in SDZB treatment
406 (Fig. 3a). Notably, no significant changes in Shannon diversity were observed with
407 individual biochar or SDZ treatments, yet their co-application significantly suppressed
408 diversity (Fig.3b). The above results indicated that SDZ enhanced biochar-induced
409 microbial carbon limitation and resulted in more serious impacts on soil microbial
410 community. The metabolism capability of carbohydrates, carboxylic acids, amino acids,
411 polymers, phenolic acid and amines significantly decreased in SDZ treatment. It was in
412 line with previous studies that showed antibiotic-mediated microbial death is a complex
413 process entailing both primary target inhibition and subsequent metabolic alterations
414 (Yang et al. 2019). Moreover, our results showed that decline in carbohydrate
415 metabolism activity directly reflected carbon-limited population crashes, while reduced
416 amino acid metabolism signaled functional shifts (Fig. 4). Enrichment analysis showed
417 that biochar amendment perturbed amino acid metabolism, particularly affecting beta-
418 alanine metabolism and arginine-proline metabolism pathways (Fig. 7). The possible
419 reason might be that microorganisms prioritize maintaining core energy metabolism
420 (such as glycolysis and the TCA cycle) and biosynthetic pathways essential for survival
421 under carbon source limitation, while simultaneously suppressing energy-intensive and
422 carbon-costly metabolic pathways like amino acid metabolism. In addition, biochar
423 application has the potential to disturb glutathione metabolism (Fig. 7). The possible
424 reason might be that soil microorganisms allocate scarce carbon resources
425 preferentially to glutathione synthesis to maintain redox homeostasis in response to the

426 strong carbon limitation, soil microorganisms allocate scarce carbon resources
427 preferentially to glutathione synthesis to maintain redox homeostasis. All the above
428 results suggested that strong microbial carbon limitation due to DOC sorption and/or
429 encapsulation by biochar served as the primary cause for the decline in microbial
430 biomass and inhibited substance metabolism, indicating suppression of native SOC
431 decomposition caused by woody biochar addition.

432 **4.3 Biochar application promoted soil carbon sequestration and stimulated the** 433 **growth of ryegrass**

434 SOC stock is regulated by the input of exogenous carbon and mineralization (Chen et
435 al., 2023). High-temperature woody biochar's direct input of stable organic carbon was
436 the primary driver of elevated SOC ceilings in this study. Moreover, the biochar-
437 induced increase in SOC storage was likely associated with the decline in SOC
438 decomposition and the stabilization of rhizodeposits and microbial necromass (Weng
439 et al. 2022). Strong DOC adsorption onto biochar transforms dissolved carbon into
440 recalcitrant organo-mineral complexes, increasing SOC stability. Furthermore, woody
441 biochar with strong adsorption capacity induced an obvious microbial carbon limitation
442 revealed by significantly decreased DOC content, further leading to decreased
443 microbial biomass. Combined with suppressed microbial carbon metabolism capability,
444 biochar had the potential to retard the mineralization of native SOC. Similarly, previous
445 studies also reported that biochar application induced negative priming effects on SOC
446 sequestration due to DOC sorption by the biochar surface (Yang et al. 2022b;
447 Viswanathan et al. 2023). And there are also studies that showed biochar-induced

448 increases in DOC can stimulate soil microbial biomass and induce short-term positive
449 priming effects (Liu et al. 2022a, Ren et al. 2022, Chen et al. 2023). Even so, if microbes
450 are competitive, they can decrease mineralization and promote SOC sequestration
451 (Chen et al., 2019). Biochar can protect SOC from microbial degradation by
452 accelerating organo-mineral formation and soil organic interfaces, thus lifting the SOC
453 ceiling (Weng et al. 2022). Our study provided clues for the mechanism that biochar-
454 induced strong microbial carbon limitation could help raise SOC storage through
455 weakened mineralization.

456 Apart from enhancing soil carbon sequestration, biochar also has potential to promote
457 plant growth. Biochar's inherent mineral composition (e.g., P, Ca, Mg, and Si)
458 constitutes a readily mobilizable nutrient pool for plants and microbiota (Hou et al.
459 2022). Moreover, the unique structures and sorption-desorption processes endow
460 biochar with additional utility as a slow-release fertilizer for plant growth with assertive
461 sorption behavior enabling concentration of soil nutrients. The porous network within
462 biochar particles and the unique interaction between nutrients and the carbon material
463 results in slow nutrient release into the aqueous phase improving plant nutrient uptake
464 (Wang et al. 2019). Furthermore, significant shifts occurred in the relative content of
465 compounds associated with ABC transporter, which actively transport diverse small
466 molecules (lipids, sugars, peptides, nutrient, etc.) across membranes in all domains of
467 life. The increased content of compounds associated with mineral and organic ion
468 transports indicated that biochar application might accelerate nutrient transport in soil.
469 The above results suggested that biochar application could prompt soil carbon

470 sequestration and boost plant growth through nutrient supply and retention.

471 **5. Conclusion**

472 Our study shed light on the biological mechanisms of biochar-induced carbon
473 sequestration and synergistic plant growth promotion. Biochar application lifted the
474 SOC ceiling, while significantly reducing DOC content due to strong adsorption.
475 Antibiotic presence could enhance this biochar-induced strong microbial carbon
476 limitation, limit the growth of soil microbes and induce weaker microbial metabolism
477 capability. Beyond its compositional nutrient supply, biochar significantly elevates soil
478 nutrient retention via its distinct physicochemical and biological properties. The
479 mechanistic understanding of negative priming effects due to DOC sorption and/or
480 encapsulation by high-temperature biochar is critical to fully assess the potential of
481 biochar application as a win-win strategy to promote plant growth and achieve carbon
482 neutrality especially in antibiotic-contaminated soil.

483 **Declaration of competing interest**

484 The authors declare that they have no conflict of interest.

485 **Author contributions**

486 Hongyan Guo and Linlin Qiu contributed to the study conception and design. Material
487 preparation, data collection and analysis were performed by Yihao Chen, Shuyu Zhou
488 and Jia Du. Data management was performed by Qingwei Zhou and Meiqing Jin. The
489 first draft of the manuscript was written by Linlin Qiu. Tim J. Daniell, Muhammad
490 Nafees, Weihong Wu, Weiyang Ji, Jiaying Ge and Hongyan Guo commented on
491 previous versions of the manuscript. All authors have read and approved the final

492 manuscript.

493 **Acknowledgments**

494 We gratefully acknowledge the financial support of the Science and Technology
495 Innovation Program of Jiangsu Province (grant numbers BK20220036), Science and
496 Technology Cooperation Plan Project in “Three Rural Issues and Nine Aspects” of
497 Zhejiang Province (grant numbers 2024SNJF066), Natural Environment Research
498 Council (grant numbers NE/N00745X/1 and NE/S009132/1), National Natural Science
499 Foundation of China (grant numbers 41571130061, 42173073 and 42277017).

500 **Reference**

- 501 Anderson M (2001) A new method for non-parametric multivariate analysis of variance.
502 *Austral Ecol* 26: 32-46. <https://doi.org/10.1111/j.1442-9993.2001.tb00081.x>.
- 503 Anderson MJ, Willis TJ (2003) Canonical analysis of principal coordinates: A useful
504 method of constrained ordination for ecology. *Ecology* 84: 511-525.
505 [https://doi.org/10.1890/0012-9658\(2003\)084\[0511:CAOPCA\]2.0.CO;2](https://doi.org/10.1890/0012-9658(2003)084[0511:CAOPCA]2.0.CO;2).
- 506 Callahan BJ, McMurdie PJ, Rosen MJ, Han AW, Johnson AJA, Holmes SP (2016)
507 DADA2: High-resolution sample inference from Illumina amplicon data. *Nat*
508 *Methods* 13: 581-583. <https://doi.org/10.1038/NMETH.3869>.
- 509 Chen LJ, Jiang YJ, Liang C, Luo Y, Xu QS, Han C, Zhao QG, Sun B (2019) Competitive
510 interaction with keystone taxa induced negative priming under biochar
511 amendments. *Microbiome* 7: 77. <https://doi.org/10.1186/s40168-019-0693-7>.
- 512 Chen W, Westerhoff P, Leenheer JA, Booksh K (2003) Fluorescence excitation-
513 emission matrix regional integration to quantify spectra for dissolved organic

514 matter. *Environ Sci Technol* 37: 5701-5710. <https://doi.org/10.1021/es034354c>.

515 Chen Y, Du Z, Weng ZH, Sun K, Zhang Y, Liu Q, Yang Y, Li Y, Wang Z, Luo Y, Gao B,
516 Chen B, Pan Z, Van Zwieten L (2023) Formation of soil organic carbon pool is
517 regulated by the structure of dissolved organic matter and microbial carbon pump
518 efficacy: A decadal study comparing different carbon management strategies.
519 *Global Change Biol* 29: 5445-5459. <https://doi.org/10.1111/gcb.16865>.

520 Chen Z, Jin P, Wang H, Hu T, Lin X, Xie Z (2022) Ecoenzymatic stoichiometry reveals
521 stronger microbial carbon and nitrogen limitation in biochar amendment soils: A
522 meta-analysis. *Sci Total Environ* 838: 156532.
523 <https://doi.org/10.1016/j.scitotenv.2022.156532>.

524 Chong J, Wishart DS, Xia J (2019) Using MetaboAnalyst 4.0 for comprehensive and
525 integrative metabolomics data analysis. *Curr Protoc Bioinf* 68: e86.
526 <https://doi.org/10.1002/cpbi.86>.

527 Feng Z, Fan Z, Song H, Li K, Cheng F (2021) Biochar induced changes of soil dissolved
528 organic matter: The release and adsorption of dissolved organic matter by biochar
529 and soil. *Sci Total Environ* 783: 147091.
530 <https://doi.org/10.1016/j.scitotenv.2021.147091>.

531 Fortuna, A.M., Marsh, T.L., Honeycutt, C.W., Halteman, W.A., 2011. Use of primer
532 selection and restriction enzymes to assess bacterial community diversity in an
533 agricultural soil used for potato production via terminal restriction fragment length
534 polymorphism. *Appl Microbiol Biotechnol* 91: 1193-1202.
535 <https://doi.org/10.1007/s00253-011-3363-7>.

536 Gao L, Wang R, Shen GM, Zhang JX, Meng GX, Zhang JG (2017) Effects of biochar
537 on nutrients and the microbial community structure of tobacco-planting soils. *J*
538 *Soil Sci Plant Nutr* 17: 884-896. [https://doi.org/10.4067/S0718-](https://doi.org/10.4067/S0718-95162017000400004)
539 [95162017000400004](https://doi.org/10.4067/S0718-95162017000400004).

540 Guenet B, Gabrielle B, Chenu C, Arrouays D, Balesdent JM, Bernoux M, Bruni E,
541 Caliman JP, Cardinael R, Chen SC, Ciais P, Desbois D, Fouche J, Frank S, Henault
542 C, Lugato E, Naipal V, Nesme T, Obersteiner M, Pellerin S, Powlson DS, Rasse
543 DP, Rees F, Soussana JF, Su Y, Tian HQ, Valin H, Zhou F (2021) Can N₂O
544 emissions offset the benefits from soil organic carbon storage? *Global Change Biol*
545 *27*: 237-256. <https://doi.org/10.1111/gcb.15342>.

546 Guo KY, Zhao YZ, Liu Y, Chen JH, Wu QF, Ruan YF, Li SH, Shi J, Zhao L, Sun X,
547 Liang CF, Xu QF, Qin H (2020) Pyrolysis temperature of biochar affects
548 ecoenzymatic stoichiometry and microbial nutrient-use efficiency in a bamboo
549 forest soil. *Geoderma* 363: 114162.
550 <https://doi.org/10.1016/j.geoderma.2019.114162>.

551 Hall M, Beiko RG (2018) 16S rRNA gene analysis with QIIME2. *Methods Mol Biol*
552 *1849*: 113-129. https://doi.org/10.1007/978-1-4939-8728-3_8.

553 Han W, Zhang M, Zhao Y, Chen W, Sha H, Wang L, Diao Y, Tan Y, Zhang Y (2024)
554 Tetracycline removal from soil by phosphate-modified biochar: performance and
555 bacterial community evolution. *Sci Total Environ* 912: 168744.
556 <https://doi.org/10.1016/j.scitotenv.2023.168744>.

557 Hou J, Pugazhendhi A, Sindhu R, Vinayak V, Thanh NC, Brindhadevi K, Lan Chi NT,

558 Yuan D (2022) An assessment of biochar as a potential amendment to enhance
559 plant nutrient uptake. *Environ Res* 214: 113909.
560 <https://doi.org/10.1016/j.envres.2022.113909>.

561 Ji X, Shen Q, Liu F, Ma J, Xu G, Wang Y, Wu M (2012) Antibiotic resistance gene
562 abundances associated with antibiotics and heavy metals in animal manures and
563 agricultural soils adjacent to feedlots in Shanghai; China. *J Hazard Mater* 235–236:
564 178–185. <https://doi.org/10.1016/j.jhazmat.2012.07.040>.

565 Kasozi GN, Zimmerman AR, Nkedi-Kizza P, Gao B (2010) Catechol and humic acid
566 sorption onto a range of laboratory-produced black carbons (biochars). *Environ
567 Sci Technol* 44: 6189-6195. <https://doi.org/10.1021/es1014423>.

568 Klindworth A, Pruesse E, Schweer T, Peplies J, Quast C, Horn M, Glöckner FO (2012)
569 Evaluation of general 16S ribosomal RNA gene PCR primers for classical and
570 next-generation sequencing-based diversity studies. *Nucleic Acids Res* 41: e1.
571 <https://doi.org/10.1093/nar/gks808>.

572 Kuzyakov Y (2010) Priming effects: Interactions between living and dead organic
573 matter. *Soil Biol Biochem* 42: 1363-1371.
574 <https://doi.org/10.1016/j.soilbio.2010.04.003>.

575 Lehmann J, Rillig MC, Thies J, Masiello CA, Hockaday WC, Crowley D (2010)
576 Biochar effects on soil biota - A review. *Soil Biol Biochem* 42: 1812-1836.
577 <https://doi.org/10.1016/j.soilbio.2010.04.003>.

578 Li F, Peng Y, Fang W, Altermatt F, Xie Y, Yang J, Zhang X (2018) Application of
579 environmental DNA metabarcoding for predicting anthropogenic pollution in

580 rivers. Environ Sci Technol 52: 11708-11719.
581 <https://doi.org/10.1021/acs.est.8b03869>.

582 Li H, Xia Y, Zhang G, Zheng G, Fan M, Zhao H (2022) Effects of straw and straw-
583 derived biochar on bacterial diversity in soda saline-alkaline paddy soil. Ann
584 Microbiol 72: 15. <https://doi.org/10.1186/s13213-022-01673-9>.

585 Lichtenthaler HK (1987) Chlorophylls and carotenoids. Pigments of photosynthetic
586 membranes. Methods Enzymol 148: 350-382. [https://doi.org/10.1016/0076-
587 6879\(87\)48036-1](https://doi.org/10.1016/0076-6879(87)48036-1).

588 Liu H, Zhao B, Zhang X, Li L, Zhao Y, Li Y, Duan K (2022a) Investigating biochar-
589 derived dissolved organic carbon (DOC) components extracted using a sequential
590 extraction protocol. Materials 15. <https://doi.org/10.3390/ma15113865>.

591 Liu M, Zhu J, Yang X, Fu Q, Hu H, Huang Q (2022b) Biochar produced from the straw
592 of common crops simultaneously stabilizes soil organic matter and heavy metals.
593 Sci Total Environ 828: 154494. <https://doi.org/10.1016/j.scitotenv.2022.154494>.

594 Liu ZT, Ma RA, Zhu D, Konstantinidis KT, Zhu YG, Zhang SY (2024) Organic
595 fertilization co-selects genetically linked antibiotic and metal(loid) resistance
596 genes in global soil microbiome. Nat Commun 15(1): 5168.
597 <https://doi.org/10.1038/s41467-024-49165-5>.

598 López-Ibáñez J, Pazos F, Chagoyen M (2016) MBROLE 2.0—functional enrichment
599 of chemical compounds. Nucleic Acids Res 44: W201-W204.
600 <https://doi.org/10.1093/nar/gkw253>.

601 Lu H, Yan M, Wong MH, Mo WY, Wang Y, Chen XW, Wang JJ (2020) Effects of

602 biochar on soil microbial community and functional genes of a landfill cover three
603 years after ecological restoration. *Sci Total Environ* 717: 137133.
604 <https://doi.org/10.1016/j.scitotenv.2020.137133>.

605 Luo L, Wang J, Lv J, Liu Z, Sun T, Yang Y, Zhu YG (2023) Carbon sequestration
606 strategies in soil using biochar: Advances, challenges, and opportunities. *Environ*
607 *Sci Technol* 57: 11357-11372. <https://doi.org/10.1021/acs.est.3c02620>.

608 Maestrini B, Herrmann AM, Nannipieri P, Schmidt MWI, Abiven S (2014) Ryegrass-
609 derived pyrogenic organic matter changes organic carbon and nitrogen
610 mineralization in a temperate forest soil. *Soil Biol Biochem* 69: 291-301.
611 <https://doi.org/10.1016/j.soilbio.2013.11.013>.

612 Moinet G, Hijbeek R, Vuuren D, Giller K (2023) Carbon for soils, not soils for carbon.
613 *Global Change Biol* 29: 2384-2398. <https://doi.org/10.1111/gcb.16570>.

614 Nelson DW, Sommers LE (1982) Total carbon, organic carbon, and organic matter. In:
615 Page AL, Miller RH, Keeney DR (eds.) *Methods of Soil Analysis, Part 2, Chemical*
616 *and Microbiological Properties*, 2nd edn. American Society of Agronomy, Inc,
617 Madison, pp. 539-579.

618 Oren A, Chefetz B (2012) Sorptive and desorptive fractionation of dissolved organic
619 matter by mineral soil matrices. *J Environ Qual* 41: 526-533.
620 <https://doi.org/10.2134/jeq2011.0362>.

621 Oyedara OO, Segura-Cabrera A, Guo X, Elufisan TO, Cantú González RA, Rodríguez
622 Pérez MA (2018) Whole-genome sequencing and comparative genome analysis
623 provided insight into the predatory features and genetic diversity of two

624 *Bdellovibrio* species isolated from soil. Int J Genomics 2018: 9402073.
625 <https://doi.org/10.1155/2018/9402073>.

626 Parks D, Tyson G, Philip H, Beiko R (2014) STAMP: Statistical analysis of taxonomic
627 and functional profiles. Bioinformatics 30: 3123-3124.
628 <https://doi.org/10.1093/bioinformatics/btu494>.

629 Paustian K, Lehmann J, Ogle S, Reay D, Robertson GP, Smith P (2016) Climate-smart
630 soils. Nature 532: 49-57. <https://doi.org/10.1038/nature17174>.

631 Qiu L, Daniell TJ, Banwart SA, Nafees M, Wu J, Du W, Yin Y, Guo H (2021) Insights
632 into the mechanism of the interference of sulfadiazine on soil microbial
633 community and function. J Hazard Mater 419: 126388.
634 <https://doi.org/10.1016/j.jhazmat.2021.126388>.

635 Qiu L, Niu L, Nafees M, Zhou S, Wu W, Du J, Zhou Q, Jin M, Guo H (2025)
636 Mechanisms for sulfadiazine effective mitigation in biochar-amended soil: From
637 antibiotic resistance to soil microbial community composition and function. J
638 Environ Manage 386: 125702. <https://doi.org/10.1016/j.jenvman.2025.125702>.

639 Quast C, Pruesse E, Yilmaz P, Gerken J, Schweer T, Yarza P, Peplies J, Glöckner FO
640 (2012) The SILVA ribosomal RNA gene database project: improved data
641 processing and web-based tools. Nucleic Acids Res 41: D590-D596.
642 <https://doi.org/10.1093/nar/gks1219>.

643 Ren CJ, Mo F, Zhou ZH, Bastida F, Delgado-Baquerizo M, Wang JY, Zhang XY, Luo
644 YQ, Griffis TJ, Han XH, Wei GH, Wang J, Zhong ZK, Feng YZ, Ren GX, Wang
645 XJ, Yu KL, Zhao FZ, Yang GH, Yuan FH (2022) The global biogeography of soil

646 priming effect intensity. *Global Ecol Biogeogr* 31: 1679-1687.
647 <https://doi.org/10.1111/geb.13524>.

648 Rhodes KA, Schweizer HP (2016) Antibiotic resistance in *Burkholderia* species. *Drug*
649 *Resistance Updates* 28: 82-90. <https://doi.org/10.1016/j.drup.2016.07.003>.

650 Sanderman J, Hengl T, Fiske GJ (2017) Soil carbon debt of 12,000 years of human land
651 use. *Proc Natl Acad Sci U.S.A.* 114: 9575-9580.
652 <https://doi.org/10.1073/pnas.1706103114>.

653 Swenson TL, Jenkins S, Bowen BP, Northen TR (2015) Untargeted soil metabolomics
654 methods for analysis of extractable organic matter. *Soil Biol Biochem* 80: 189–
655 198. <https://doi.org/10.1016/j.soilbio.2014.10.007>.

656 Tan S, Narayanan M, Thu Huong DT, Ito N, Unpaprom Y, Pugazhendhi A, Lan Chi NT,
657 Liu J (2022) A perspective on the interaction between biochar and soil microbes:
658 A way to regain soil eminence. *Environ Res* 214: 113832.
659 <https://doi.org/10.1016/j.envres.2022.113832>.

660 Viswanathan SP, Njzhakunnathu GV, Neelamury SP, Padmakumar B, Ambatt TP
661 (2023) Invasive Wetland Weeds Derived Biochar Properties Affecting Soil Carbon
662 Dynamics of South Indian Tropical Ultisol. *Environ Manage* 72: 343–362.
663 <https://doi.org/10.1007/s00267-023-01791-3>.

664 Wang B, Zhang Y, Zhu D, Li H (2020) Assessment of bioavailability of biochar- sorbed
665 tetracycline to *Escherichia coli* for activation of antibiotic resistance genes.
666 *Environ Sci Technol* 54 (20): 12920–12928. [https://doi.org/10.1021/acs.](https://doi.org/10.1021/acs.est.9b07963)
667 [est.9b07963](https://doi.org/10.1021/acs.est.9b07963).

668 Wang Y, Villamil MB, Davidson PC, Akdeniz N (2019) A quantitative understanding
669 of the role of co-composted biochar in plant growth using meta-analysis. *Sci Total*
670 *Environ* 685: 741-752. <https://doi.org/10.1016/j.scitotenv.2019.06.244>.

671 Weng ZH, Van Zwieten L, Tavakkoli E, Rose MT, Singh BP, Joseph S, Macdonald LM,
672 Kimber S, Morris S, Rose TJ, Archanjo BS, Tang C, Franks AE, Diao H,
673 Schweizer S, Tobin MJ, Klein AR, Vongsvivut J, Chang SLY, Kopittke PM, Cowie
674 A (2022) Microspectroscopic visualization of how biochar lifts the soil organic
675 carbon ceiling. *Nat Commun* 13: 5177. [https://doi.org/10.1038/s41467-022-](https://doi.org/10.1038/s41467-022-32819-7)
676 [32819-7](https://doi.org/10.1038/s41467-022-32819-7).

677 Withers E, Hill PW, Chadwick DR, Jones DL (2020) Use of untargeted metabolomics
678 for assessing soil quality and microbial function. *Soil Biol Biochem* 143: 107758.
679 <https://doi.org/10.1016/j.soilbio.2020.107758>.

680 Wu J, Joergensen RG, Pommerening B, Chaussod R, Brookes PC (1990) Measurement
681 of soil microbial biomass C by fumigation-extraction—an automated procedure.
682 *Soil Biol Biochem* 22: 1167-1169. [https://doi.org/10.1016/0038-0717\(90\)90046-](https://doi.org/10.1016/0038-0717(90)90046-3)
683 [3](https://doi.org/10.1016/0038-0717(90)90046-3).

684 Yang JH, Wright SN, Hamblin M, McCloskey D, Alcantar MA, Schrübbers L, Lopatkin
685 AJ, Satish S, Nili A, Palsson BO, Walker GC, Collins JJ (2019) A white-box
686 machine learning approach for revealing antibiotic mechanisms of action. *Cell* 177
687 (6): 1649–1661. <https://doi.org/10.1016/j.cell.2019.04.016>.

688 Yang Y, Sun K, Han L, Chen Y, Liu J, Xing B (2022a) Biochar stability and impact on
689 soil organic carbon mineralization depend on biochar processing, aging and soil

690 clay content. Soil Biol Biochem 169: 108657.

691 <https://doi.org/10.1016/j.soilbio.2022.108657>.

692 Yang Y, Sun K, Liu J, Chen Y, Han L (2022b) Changes in soil properties and CO₂

693 emissions after biochar addition: Role of pyrolysis temperature and aging. Sci

694 Total Environ 839: 156333. <https://doi.org/10.1016/j.scitotenv.2022.156333>.

695 **Figure Captions**

696 Fig. 1. Effects of SDZ presence and biochar application on ryegrass growth. (a) biomass

697 of ryegrass, (b) root length of ryegrass, and (c) photosynthetic pigments of ryegrass

698 leaves. Error bars are standard deviations of the mean of four independently prepared

699 samples. Different letters over bars denote significant differences ($P < 0.05$).

700 Fig. 2. Changes in soil organic carbon due to SDZ presence and biochar application. (a)

701 the content of SOC and (b) DOC, (c) fluorescence region integral results indicate DOC

702 compositions of soil.

703 Fig. 3. Variations in bacterial community on account of SDZ presence and biochar

704 application. (a) microbial biomass estimated by microbial biomass carbon, (b) alpha

705 diversity estimated by Shannon index, (c) PCoA plot of bacterial community

706 composition based on Bray-Curtis metric distance, (d) bar plots of bacterial community

707 composition at class taxonomic levels, and extended error bar plot of distinct genera

708 between (e) CK and B treatment and (f) CK and SDZB treatment based on Welch's t-

709 test with Benjamini-Hochberg FDR produces at p-value < 0.05 .

710 Fig. 4. Changes in soil (a) microbial carbon metabolism capability estimated by the

711 average well color development (AWCD) and (b) normalized microbial carbon

712 metabolism capability estimated by the value of AWCD relative to MBC due to SDZ
713 presence and biochar application.

714 Fig. 5. Changes in soil metabolites after biochar application revealed by untargeted
715 metabolomics. Bar plots of the relative content of compounds with different
716 classification, (a) carbohydrates, (b) amines, (c) amino acids, (d) organic acids, (e) fatty
717 acids, and (f) PCA plot of soil metabolites composition based on Bray-Curtis metric
718 distance.

719 Fig. 6. Cluster heatmap of normalized peak areas for top 50 soil metabolites which were
720 significantly changed after biochar application. Metabolite row groups were colored by
721 the classification they belong to. The color of metabolite name indicated the
722 classification of the involved pathway. The pink indicated carbohydrate metabolism,
723 the orange indicated amino acid metabolism, the purple indicated lipid metabolism and
724 the blue indicated nucleotide metabolism.

725 Fig.7. The potentially perturbed biological pathways in response to SDZ presence and
726 biochar application which was drawn based on KEGG database. (a) ABC transporters,
727 (b) beta-alanine metabolism, (c) Glutathione metabolism, (d) Arginine and proline
728 metabolism. The color of soil metabolites indicated that the relative content increased
729 (orange) or decreased (green) owing to biochar application with the absence and
730 presence of SDZ in soil.

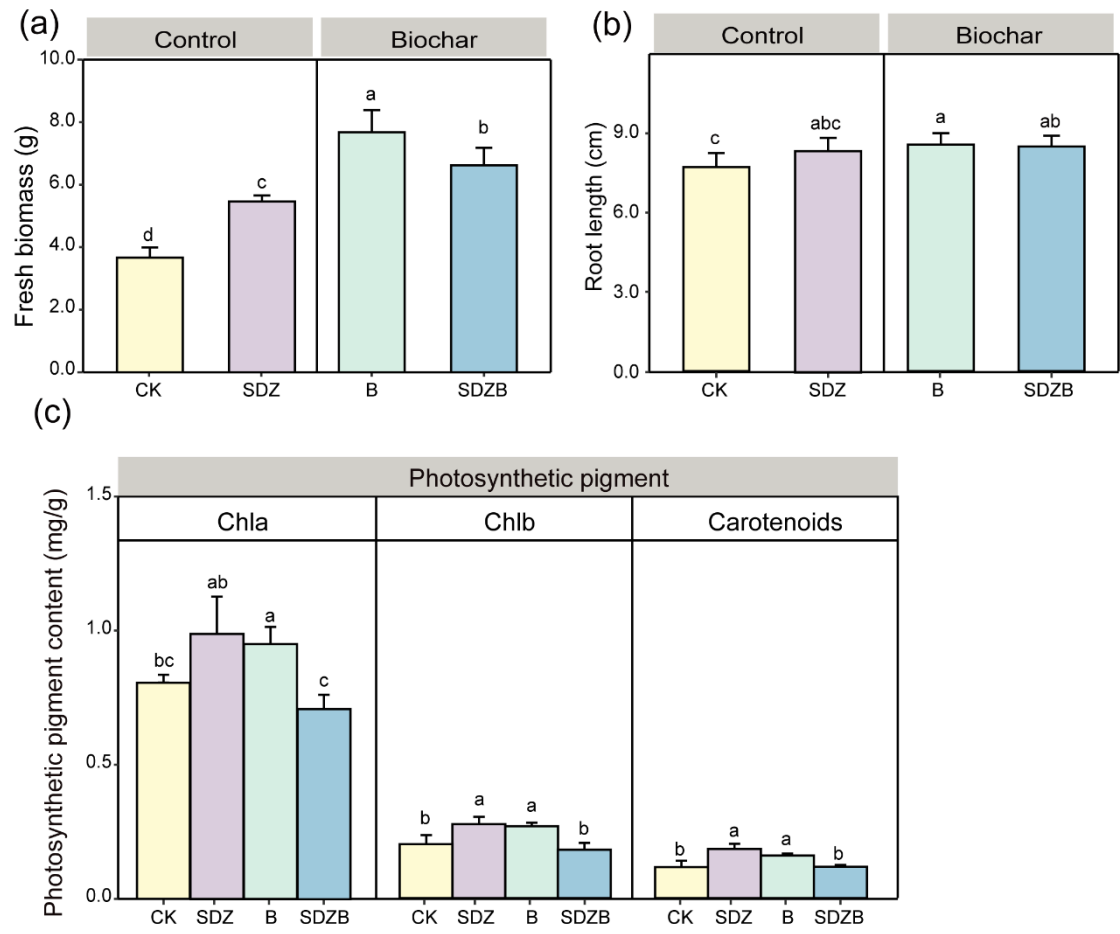


Fig. 1

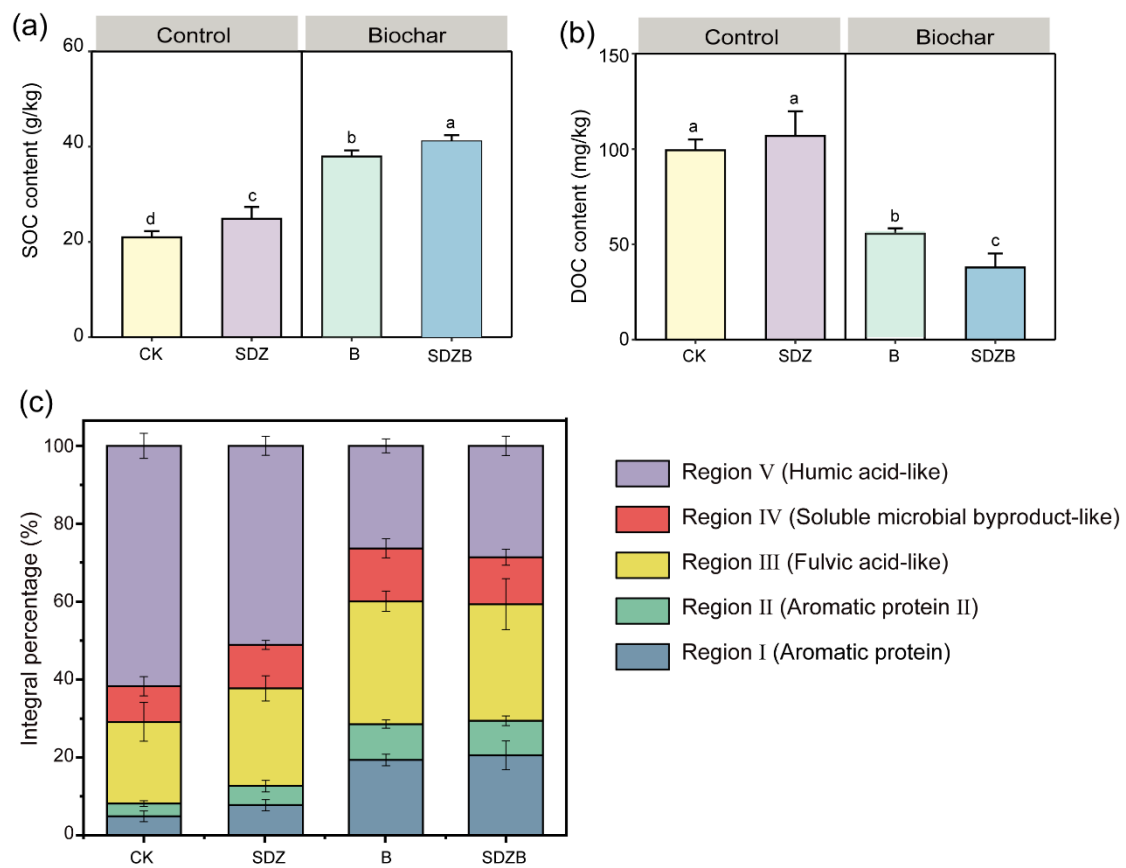


Fig. 2

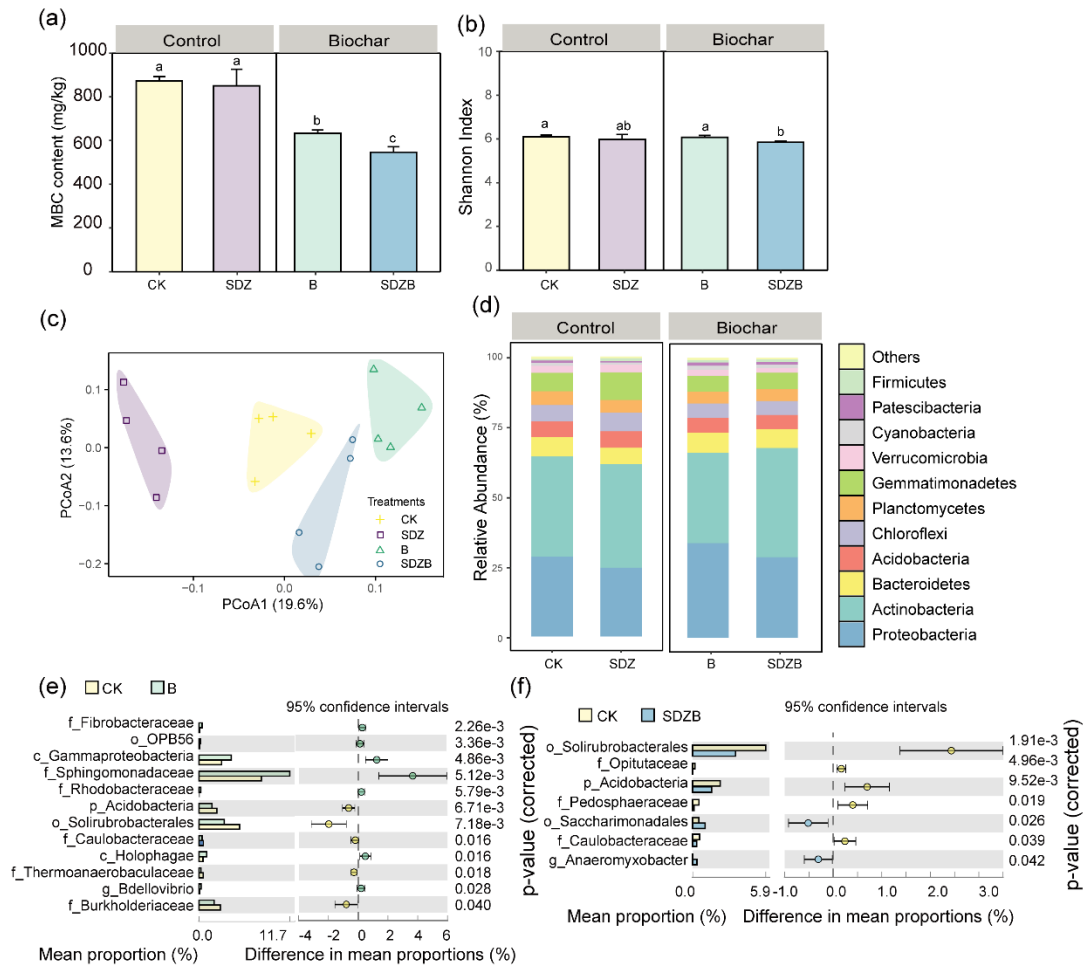


Fig. 3

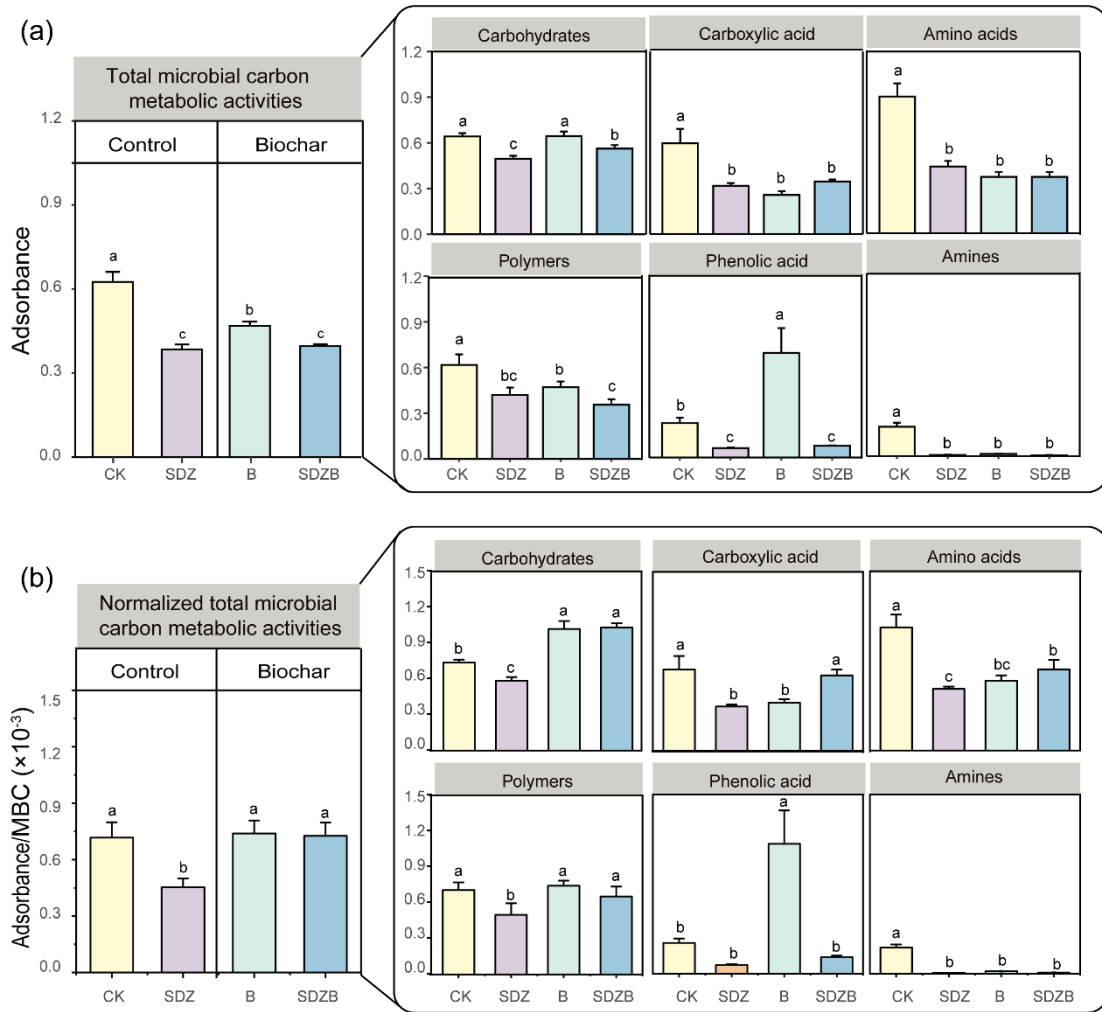


Fig. 4

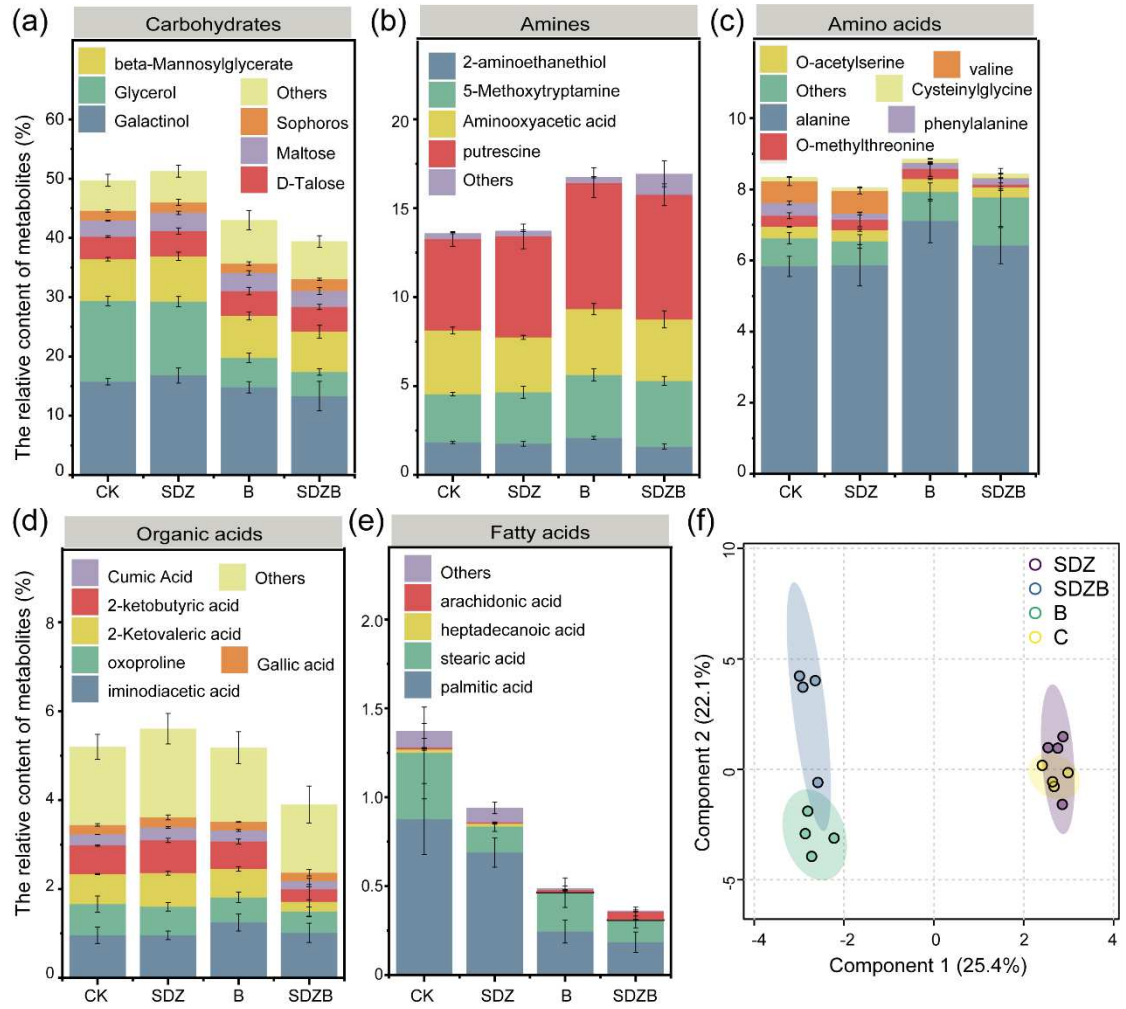


Fig. 5

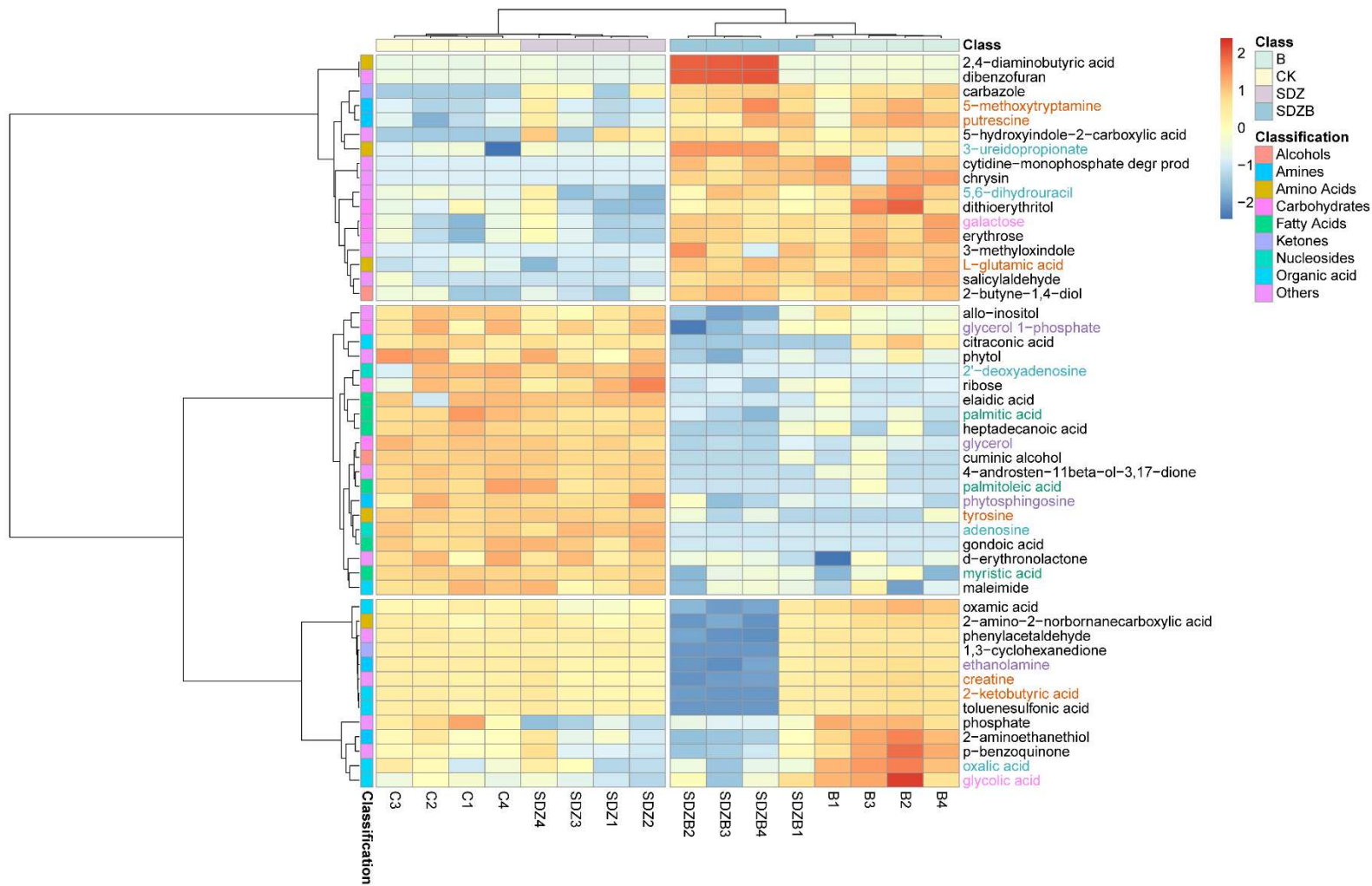


Fig. 6

